Submitted to *Materials Science and Engineering A*
December 2006

Mechanical Characterization of Poly(L-lactide) and Poly(methyl methacrylate) Blends

Kim-Phuong Le[a], *Richard Lehman*[a,*], *Kenneth VanNess*[b], *Michelle Dickinson* [c]

[a]AMIPP Advanced Polymer Center, Rutgers University, Piscataway, NJ 08854.

[b]Department of Physics, Washington and Lee University, Lexington, VA

[c]Hysitron, Inc., 10025 Valley View Road, Minneapolis, MN 55344

Corresponding Author:

Richard L. Lehman
Professor of Materials Engineering
Rutgers University
607 Taylor Road, Piscataway, New Jersey 08854-8065
Phone: 609.203.2501; fax: 732.445.5584; email: rllehman@rutgers.edu

Abstract

PLLA/PMMA blends, which are of interest as in-vivo biomaterials due to their biocompatibility and differential resorbability, were studied with respect to selected mechanical properties. These blends are immiscible and the mechanical properties of the intermediate compositions, particularly the co-continuous compositions near the phase inversion point, are critical to biomedical engineering design. Overall, results show that the mechanical properties of these compositions are quite good, as measured by a variety of methods. Tensile modulus increased 22% and fracture strength 15%. Flexural modulus was 7-8% above the proportional value. Dynamic measurements at the glass transition revealed enhanced modulus (storage) around the phase inversion where the modulus was increased >70%. Unusual glass transition data were measured by DMA that seem to indicate an unexpected drop in PMMA glass transition as small to moderate amounts of PLLA are added, supporting other corroborating DSC studies. Preliminary nanoindentation measurements show that blends in this system have higher storage modulus and higher loss modulus than neat PMMA. Overall, this system possesses well bonded interfaces, capable of excellent load transfer, and some degree of polymer molecular orientation that enables synergistic Young's modulus values in co-continuous blends.

Keywords: polymer blend, extrusion, miscibility, synergy

Introduction

The multiphase Poly(L-lactide) (PLLA)/Poly(methyl methacrylate) (PMMA) blend was originally studied in our laboratory as a biomimetic system for targeted biomedical applications such as bone fillers or bone grafts. In theory, blends of PLLA and PMMA should form an immiscible polymer system and, in biological environments, provides a unique material where one phase is degradable and responsible for material-tissue integration while the other phase is persistent and responsible for structural integrity [1]. The ideal balance of mechanical properties and biodegradability in such system depends on the end application and this balance can be achieved by varying the molecular weight of the starting polymers, the composition of the blend, the processing parameters – most importantly temperature and shear rate, and post-processing thermal and chemical treatment [1-4].

Although immiscible polymer blends are used in increasing number of diverse commercial applications, the bonding of the interface, either via compatibilizers or mechanical grafting [5] is always a concern. Biomedical applications are no exception and a weak interface will have adverse effects on the mechanical properties of the blend [4], both initially and during in-vivo degradation. Previous work from our laboratory [1, 6] has shown that the PLLA/PMMA system is special in that thermal extrusion and compression molding of high molecular weight PLLA and PMMA results in a multiphase structure where an alloy-like phase with a characteristic intermediate glass transition temperature near 80 ^{o}C is formed in the blends regardless of starting resins. Similar observations on the intermediate glass transition have recently been reported by others [7, 8], suggesting partial miscibility in PLLA/PMMA system. The new phase, termed PG80, occurs at the interface and renders self-compatibilizing ability to the blend. If the system is indeed self-compatibilized by PG80, then its mechanical properties such as tensile modulus

should follow rule of mixtures behavior at co-continuous composition due to bonding and load transfer across the phase boundaries [9]. One of the blend components, semi-crystalline PLLA, is known as an orientable polymer [10] and synergisms above the rule of mixtures may also be possible if some degree of morphological orientation occurs in combination with self-compatibilization.

In this study, PLLA/PMMA blends were prepared via thermal processing over a full range of blend compositions and selected mechanical properties were examined to determine if the self-compatibilizing phase, PG80, is capable of transferring load between the PLLA and PMMA phases to produce near rule of mixtures behavior. Mechanical properties which are greater than the rule of mixtures would be an indication of partial orientation of PLLA structures in the blend.

Experimental:

Materials

Extrusion-grade PMMA pellets were obtained from Atofina Chemicals Inc., Philadelphia, PA, USA, and medical-grade of poly(L-lactide) (PLLA), Purasorb® PL was obtained in the form of white granular powders from Purac America, Lincolnshire, IL, USA.

Extrusion

Rheology measurements were performed on both polymers using a TA AR 2000 rheometer [TA Instruments, New Castle, DE, U.S.A] over a range of shear rates for relevant temperatures. The data were used to predict the composition range over which co-continuous blends are expected[1]. The PLLA/PMMA composition that conforms to this co-continuous compositional relationship is 45 volume percent for Purasorb® PL as shown in Table I.

The PLLA and PMMA polymers were dried for 48 hours in a vacuum oven (30 mmHg) at 45 °C and 70 °C, respectively, prior to processing. Batches of 140-g were weighed out and melt processed in a 19-mm single screw laboratory extruder [C. W. Brabender, Inc., Hackensack, NJ] fitted with a mixing screw of 16.64 mm average root diameter. An average shear rate of 39.25 s^{-1} was achieved at 200 ^{o}C by operating the extruder at 50 revolutions per minute. A 20/100/20 screen pack was installed after the barrel and before the 3.18 -mm die nozzle.

Tensile Mechanical Testing

Thin films (200 ± 20 μm) of PLLA/PMMA blends were pressed from extruded rod at 200 °C using a Carver hydraulic press [Carver, Inc., Wabash, IN, USA]. Highly polished chrome-coated stainless steel plates of 1-mm thickness were used to clad the heated platens to produce films with good surface finish. Total pressing time for each sample was 3 minutes, and the plates were cooled in air to room temperature prior to de-molding. The films were visually examined for defects and defect-free films were cut into 8 mm x 3 mm rectangular strip with a sharp surgical blade. Care was taken to make a clean cut and to avoid generating defects on the edges that could adversely affect the property measurements. All strips were conditioned in ambient condition for 48 hours prior to testing.

Tensile test were performed at room temperature [22 ^{o}C] and approximately 50% relative humidity on a MTS 2000 [MTS Inc., Eden Prairie, MN] tensile testing instrument. The initial gage length, i.e. the distance between the grips, was 50 mm. To prevent slippage and/or failure at the grip, the MTS 100-N Vise-Action grip set was installed on a 500-N load cell. This grip set is especially designed for fiber and film work and a hard rubber-like compound coats the grips to minimize slippage or damage to the test specimen. The test speed was 5 millimeters per minute and the data acquisition rate was 10 Hertz. . The initial slope of the stress-strain curve was

reported as the tensile modulus. Ultimate tensile strength and fracture stress were determined at peak load and failure load points respectively. No yield point was identified in these materials.

Flexural DMA

Dynamic mechanical analysis [DMA 7E, Perkin-Elmer, Wellesley, MA] was used to determine the flexural modulus of the blends in 3-point bending. A custom extension was devised to accommodate the testing of cylindrical extruded rods with 4.70-mm average diameter and 80-mm span. Dynamic stress scans at room temperature under calculated force rate to ensure a uniform constant stress force of 395 KPa on all test specimens. This constant stress force was selected so that the instrument could operate below its maximum force rate of 0.250 N/min. The DMA 7E software used a correction factor of 2.998. Five specimens at each composition were tested, and average flexural modulus was reported.

Torsional DMA

Dynamic mechanical analysis (DMA) was also performed on rectangular specimens molded with the Carver press at 200 ^{o}C from extruded rods that measured 60 mm x 12 mm x 1 mm. The specimens were run on an AR-2000 rheometer [TA Instruments, New Castle, DE] in torsional mode. All tests were conducted in an environmentally-controlled test chamber in which the specimens were heated in nitrogen from 25 ^{o}C to 120 ^{o}C at 2 ^{o}C/min at 5 and 30 Hz. Liquid nitrogen was used for precise temperature control. The strain rate was selected based on linear viscoelastic region (LVR) test to be 0.05 %. Glass transition temperatures were indicated by the maxima of the loss modulus (G") signal curves.

Modulus Mapping via Nanoindentation

Selected short cylinders were also taken from the extruded rods using a saw blade, embedded in epoxy, allowed curing overnight at 40 ^{o}C inside a temperature-controlled chamber [Isotemp® Oven, Fisher Scientific, Pittsburgh, PA, USA], polished and cleaned for modulus mapping using the Hysitron Triboindenter [Hysitron, Minneapolis, MN].

Modulus mapping were performed at frequency of 200 Hz and dynamic force of 0.3 µN using a Berkovich tip, 100 nm in radius, on a 50 µm by 50 µm area at 256 x 256 resolution or a total of 65, 536 test on each single image. Tip calibration was performed using fused quartz with known hardness and reduced modulus at the same frequency and scan size. Raw data including force, phase, and amplitude were collected. Machine corrections were applied using nano-DMA Tribo software [Hysitron, Minneapolis, MN] to yield tan delta, loss stiffness and storage stiffness. Complex modulus, loss modulus, and storage modulus were then calculated with correction made to the tip area using the same software.

Results and Discussion

Morphology

PLLA/PMMA is an immiscible polymer system when melt processed and the resulting two-phase composite structure exhibits a micron scale morphology (figure 1) in which the phases are distinct but mechanically compatible in that very little interface is observed in unetched specimens (figure 1a). In fact, these composites are optically clear and show little visual evidence of phase boundaries or crystallinity [11]. The compositions near the phase inversion point are co-continuous and the micrograph of an etched specimen [1] clearly shows the interesting morphologies generated by melt processing in this immiscible blend system. Although these architectures clearly have potential use as biomaterials, the effect of processing

PLLA and PMMA into these fine interconnected blend structures on the resultant mechanical properties is unclear. Certainly the close proximity of the phases, the virtually identical elastic modulus of the components, and the possibility of self-compatibilization should contribute to nearly rule of mixtures properties. The tendency of PLLA to molecularly orient as it is drawn into a co-continuous structure may impart further mechanical benefits. Resolving these questions was a major motivation for this study.

Tensile modulus and strength

The tensile stress/strain behavior of these blends followed expected behavior in which a short elastic region was followed by an extended nonlinear region (figure 2a). Ultimate tensile strength was reached near 70 MPa and fracture occurred soon thereafter. No distinct yield point was observed. All of the results in this paper are engineering stress and strain, meaning that the reduction in specimen cross section during the test was not measured or accounted for in the calculations. Thus, the slight negative curvature of the stress-strain curve may arise totally or in part from Poisson's ratio effects. Young's modulus is measured a the beginning of the curve to minimize underestimation of the value.

The tensile properties of these composites display some interesting relationships as shown in figure 2b. All compositions exhibit Young's modulus and fracture strength greater than or equal to the rule of mixtures and the properties in the vicinity of the co-continuous compositions are synergistic, i.e. well above the rule of mixtures. The maximum Young's modulus is 22.5% above the rule of mixtures and the fracture strength is 15% higher. These are commercially important but curious results since simple composite models cannot explain synergistic behavior, even in the presence of a perfectly bonded interface. Effects that may lead to synergism include

residual stress and molecular orientation. Studies of these effects is beyond the scope this paper but will certainly constitute interesting subsequent study.

Flexural modulus

Flexural stress-strain curves were linear (figure 3a) and modulus values (figure 3b) followed a behavior similar to the synergistic tensile results, although the magnitude of the flexural effect is less. The tensile modulus was about 22% above the rule of mixtures at the point of maximum synergy, whereas the flexural synergy is only 7 – 8%. The flexural test is a mechanically more complicated test with tensile, compressive, and shear components, and the amount of material under maximum tensile stress was quite less than in the tensile testing. The smaller gage region appears to be responsible for the higher maximum modulus values, 3.89 GPa in flexure compared to 2.24 GPa in tension.

Torsional DMA

Further studies of Young's modulus were conducted with torsional DMA as described in the experimental section. This segment of the work enabled the complex modulus to be resolved into storage modulus, loss modulus, and loss angle. The effect of temperature on these values and a mechanical determination of the glass transition were other benefits of this approach. Figures 4 – 6 present the results obtained from various PLLA/PMMA blends. The general DMA behavior (fig 4a,b) at 5 and 30 Hz is typical of polymer systems with the storage modulus slowly decreasing with temperature until the glass transition is reached at which point the storage modulus drops quickly and the loss modulus and loss angle respond predictably. Frequency has a significant effect on the position of the three curves since the viscoelastic relaxation times for polymers in the vicinity of the glass transition determine the degree to which the polymer can respond to applied strain. Some molecular relaxation processes that can easily accommodate a 5

Hz frequency oscillation have difficulty responding to the faster 30 Hz oscillations. Thus, the DMA curves are displaced to higher temperatures as the frequency is increased. Aside from this expected behavior, no unusual frequency effects are noted in this blend system.

The glass transition of blends ranging from 10 – 60% PLLA (volume) were determined from the DMA data and summarized in figure 5. Of the several ways to determine glass transition from these data, we selected the temperature at which the loss modulus curve was at a maximum since this method was simple and not subject to complicated algorithms or operator judgment that could introduce errors. Generally, the glass transitions of the blends follow two linear composition relationships, one defined by PLLA as the continuous phase and one defined by PMMA as the continuous phase. These lines intersect close to the phase inversion point at 41% PLLA. The effect of frequency is simply to displace the values to higher temperature, as expected.

The behavior of PLLA-rich blends follows the expected trend of nearly constant T_g as a dispersed phase of higher T_g material (PMMA) is added. The PLLA continuous phase dominates the T_g behavior until a large amount of dispersed PMMA finally begins to slightly alter the T_g. Quantitatively for this part of the 5 Hz diagram, the neat PLLA shows a T_g of 58.4 ^oC and the addition of 50% (volume) of PMMA to the PLLA only increased the T_g by 6.8 ^oC. At the other end of figure 5 more unusual behavior is observed. As small amounts of PLLA are added to PMMA, we expected the T_g to again remain nearly constant as small droplets of low T_g PLLA are dispersed in PMMA. Then, as the phase inversion point is reached we anticipated a rapid changeover to the PLLA continuous behavior as suggested by the gray dotted S-curve in figure 5. Instead, small amounts of PLLA immediately begin to reduce the T_g of the continuous PMMA phase as shown by the data. In fact, PLLA generated such a precipitous drop in T_g of the

blend that when 30% PLLA is present, the T_g has dropped 27 ^oC from 100.3 to 73.4 ^oC. DSC and Raman studies of this system show that PLLA alters the structure of PMMA in these blends, apparently promoting chain scission and oligomer formation [12]. The unusual DMA Tg effects shown in this work parallel the shift of DSC PMMA T_g to lower temperatures in the presence of PLLA.

The DMA storage modulus (measured at T_g) versus composition curve (figure 6a) compares favorably with the Young's modulus curve from tensile data (figure 2b), although the blend synergism is more pronounced in the DMA data and the DMA modulus is about a factor of four less than the maximum tensile Young's modulus. These lower values result, of course, from the fact that the data were collected at T_g. The loss modulus versus composition curve (figure 6b) was also assembled from values measured at T_g. Neat PLA exhibits higher mechanical loss at T_g than PMMA, which may be due to its semi-crystalline structure, but the key point is the overall lossier nature of the blends. Clearly the two phase structure of the blends, particularly the high interface area blends near the co-continuous composition, have difficulty keeping up with the dynamic torsional strain and lag behind as loss modulus.

Nanoindentation

To complement the tensile, flexural, and dynamic modulus measurements, several preliminary nanoindentation measurements were made on a polished sample of 35% PLLA blend and compared to a polished PMMA control. The goal was to see if the higher modulus measured by traditional means for the blends near the phase inversion composition could be supported by sub-micron indenter measurements. A secondary objective was to determine if blend morphological features could be revealed through modulus mapping.

Modulus (storage and loss) mapping of 50 μm square regions of the 35% PLLA blend (figure 7a) shows a nondescript texture with both storage and loss modulus varying over certain ranges. The modulus morphology appears to contain some surface preparation features but also certainly has some randomly distributed peaks and valleys associated with the blend structure. To achieve a more quantitative assessment and to resolve the fine structure revealed in the 50 μm square region, a line scan was made in a smaller 12 μm square as shown by the line and box in figure 7a. The storage modulus and loss modulus measured along this line scan (figure 7b) reveals the relative level of storage and loss modulus and the spatial variation of each. The storage modulus averages 15.3 GPa, a high value compared to the tensile and flexural values, but comparable to values measured on ABS [13] considering the more rubbery nature of the ABS copolymer. Furthermore, since an extremely small volume of the material is subject to the indent, i.e. the "gage" length is quite small, high values are not unexpected. Loss modulus values are low, around 1 GPa.

To compare storage modulus values in a blend with that of one end-member, and to assess whether the modulus morphology observed is real, a sample of neat PMMA was run under identical conditions (figure 7c). PMMA, known for it amorphous nature and smooth surface, generated a storage modulus of 8.5 GPa, considerably lower than that of the blend, and exhibited modulus texture much less than the blend. Studies on high modulus nitride films [14] have shown that nanoindentation gives elastic modulus reproducibility of ±12%. Applying this value to the storage modulus data (dotted lines) shows that the modulus variability for PMMA is within this limit whereas the 35% PLLA blend exhibits excursions well beyond these limits. Thus, these excursions represent real modulus texture in the blends on a scale of the order of several microns. PMMA exhibits no measurable loss modulus.

Thus, although much more complete nanoindentation work needs to be done on this system, there are sufficient data in this study to conclude that PLLA/PMMA blends exhibit elevated, synergistic nano-modulus at the 35% PLLA blend composition compared to at least one of the end-members, PMMA. Furthermore, the blend shows a higher level of modulus morphology, apparently a real feature of these blends, which needs further exploration. The blend composition also showed a loss modulus, unlike the PMMA, which is an expected feature of immiscible polymer blends.

Summary and Conclusions

PLLA/PMMA blends are immiscible and form two-phase composites that become co-continuous near the phase inversion point. Tensile modulus and fracture strength measurements indicate a maximum 22% increase in elastic modulus in these blends over the rule of mixtures value and a 15% maximum increase in fracture strength. Similar synergy was observed in flexural measurements, although the modulus increase was less (7-8%). Dynamic measurements at the glass transition temperature also showed a substantially enhanced modulus (storage) around the phase inversion where the modulus was increased >70% compared with a rule of mixtures baseline. Unusual composite glass transition data were measured by DMA that seem to indicate a unexpected drop in PMMA glass transition as small to moderate amounts of PLLA are added, supporting other corroborating DSC studies that suggest the formation of an in-situ compatibilizer. Preliminary nanoindentation measurements reveal a modulus mapping profile with features, although correlation of these features with image analysis has not yet been conducted. The nanoindent data do show that blends in this system have higher storage modulus and higher loss modulus than neat PMMA.

These results support the premise that the blend interfaces are well bonded and capable of load transfer, and that some degree of polymer orientation is occurring that permits Young's modulus values to significantly exceed the rule of mixtures value.

Acknowledgements

The authors wish to thank the AMIPP Advanced Polymer Center at Rutgers University and the New Jersey Commission on Science and Technology for supporting this work. Special thanks and appreciation go to Professor Adrian Mann of Rutgers University for assisting in the nanoindentation assessment and analysis.

References

1. Le K-P, Lehman R, Remmert J, VanNess K, Ward P-M, and Idol J, Multiphase Blends from Poly (L-lactide) and Poly (methyl methacrylate). J. Biomater. Sci. Polymer Edn, 2006. 17(1-2): p. 121-37.

2. Washburn N, Simon C, Tona A, Elgendy H, Karim A, and Amis E, Co-extrusion of biocompatible polymers for scaffolds with co-continuous morphology. J Biomed Mater Res, 2002. 60: p. 20-19.

3. Parazin P and Favis B, Morphology Control in Co-continuous Poly(L-lactide)/Polystyrene Blends: A Route towards Highly Structured and Interconnected Porosity in Poly(L-lactide) Materials. Biomacromolecules, 2003. 4(6): p. 1669-1679.

4. Dell'Erba R, Groeninckx G, Maglio G, Malinconico M, and Migliozzi A, Immiscible polymer blends of semicrystalline biocompatible components: thermal properties and phase morphology analysis of PLLA/PCL blends. Polymer, 2001. 42: p. 7831-7840.

5. Joshi J, Lehman R, Nosker T, Selected Physical Characteristics of Polystyrene/High Density Polyethylene Composites Prepared from Virgin and Recycled Materials. Journal of Applied Polymer Science, 2006. 99(5): p. 2044-2051.

6. Le K-P, Lehman R, VanNess K, and Idol J, Biomimetic Polymers and Gels - Characterizations of Multiphase Biogenic Polymer Blends from Poly(L-lactide) and Poly(methyl methacrylate). in MRS Fall Meeting. 2005. Boston, MA.

7. Shirahase T, Komatsu Y, Tominaga Y, Asai S, and Sumita M, Miscibility and hydrolytic degradation in alkaline solution of poly(L-lactide) and poly(methyl methacrylate) blends. Polymer, 2006. 47: p. 4839-4844.

8. Eguiburu J, Iruin J, Fernadez-Berridi M, and San Roman J, Blends of amorphous and crystalline polylactides with poly(methyl methacrylate) and poly(methyl acrylate): a miscibility study. Polymer, 1998. 39(26): p. 6891-6897.

9. Willemse R, Speijer A, Langeraar A, and Posthuma de Boer A, Tensile moduli of co-continuous polymer blends. Polymer, 1999. 40: p. 6645-6650.

10. Lee J, Lee K, and Jin B, Structure development and biodegradability of uniaxial stretched poly (L-lactide). European Polymer Journal, 2001. 37: p. 907-914.

11. Le K-P, Lehman R, Idol J, and Ward P-M, Biomimetic Morphologies in Synthetic Polymers via Melt Processing of Co-continuous Immiscible Polymer Blends, in Gordon Research Conference on Biomaterials: Biocompatibility/Tissue Engineering. 2003: The Holderness School, Holderness, NH, US.

12. Le K-P, Lehman R, Mann A, Idol J, Raman Characterization in Blends of Poly(L-lactide) and Poly(methyl methacrylate), in Applied Spectroscopy. 2006.

13. Dickinson M and Turek J, (2006) Modulus Mapping of a Polymer Blend. Hysitron Technical Service Publication

14. Lee J-W, Huang J-C, and Duh J-G, Nano Mechanical Properties Evaluation of RF Magnetron Sputtered Chromium Nitride Thin Film. Tamkang Journal of Science and Engineering, 2004. 7(4): p. 237-240.

15. Lu L and Mikos A, Poly(lactic acid). Polymer Data Handbook [Website] 1999 [cited 2003 03/10]; Available from: http://www.oup-usa.org/pdh.

16. Hsu S Poly(methyl methacrylate). Polymer Data Handbook [Website] 1999 [cited 2003 3/10]; Available from: http://www.oup-usa.org/pdh.

Table I. Viscosity data measured from Rheometer AR-2000 to be used to predict co-continuous compositions (200 ^{o}C)

Raw Materials:	**PLLA**	**PMMA**
Density (g/cm^3)	1.275	1.18
Viscosity (Pa.s)	4828	5844
η(PLLA) / η(PMMA)	0.826	
Co-continuous composition, volume percent PLLA	45.2	

Note: Viscosity values in this table were obtained at T = 200 ^{o}C and γ = 39.25 s^{-1}

Table IIa: Mechanical properties of raw PLLA and PMMA (Literature)[15, 16]

	PLLA	**PMMA**
Tensile Modulus (GPa)	3-4	3.1
Tensile Strength (MPa)	50-60	70
Flexural Modulus (GPa)		3.1
Flexural Strength (MPa)		103

Table IIb: Mechanical properties of thermal processed PLLA and PMMA

	PLLA	**PMMA**
Tensile Modulus (GPa)	1.550 ± 0.085	1.949 ± 0.037
Tensile Strength (MPa)	68 ± 5	68 ± 3
Flexural Modulus (GPa)	3.508 ± 0.061	3.670 ± 0.011

Figure Captions:

Figure 1a: 25/75 % (v/v) [Purac] PLLA/PMMA composite, sectioned perpendicular to extrusion axis, cryogenic fractured, un-etched, gold coated, 4 kV

Figure 1b: 28/72 % (v/v) PLLA/PMMA composite; DMF etched, sectioned perpendicular to extrusion axis

Figure 2a. Representative tensile stress-strain curve for PLLA/PMMA film specimens. This curve is for 60% PLLA by volume.

Figure 2b: Tensile modulus and fracture strength of PLLA/PMMA blends

Figure 3a. Representative flexural stress-strain curve for PLLA/PMMA rod specimens. This curve is from 50% blend

Figure 3b. Flexural modulus of PLLA/PMMA blends from 3-point bending on extruded rods.

Figure 4a: Modulus and loss angle curves by torsional DMA at 5 Hz for 45/55 PLLA/PMMA blend.

Figure 4b: Modulus and loss angle curves by torsional DMA at 30 Hz for 45/55 PLLA/PMMA blend.

Figure 5: Glass transition of blends as measured by torsional DMA

Figure 6a: Storage modulus of PLLA/PMMA blends at the glass transition.

Figure 6b: Loss modulus of PLLA/PMMA blends at the glass transition.

Figure 7a. Loss modulus map by nanoindentation on clean polished cross session of extruded polymer blend rod, 35% PLLA by volume. Dark areas are low modulus, bright areas are high. Line is location of line scan in figure 7b and the 12 μm square is the area of enlargement in 7b.

Figure 7b. Modulus line scan from location shown in 7a. Solid horizontal line is mean storage modulus and dotted lines are ±12%

Figure 7c. Modulus line scan for neat PMMA control. Solid horizontal line is mean storage modulus and dotted lines are ±12%.

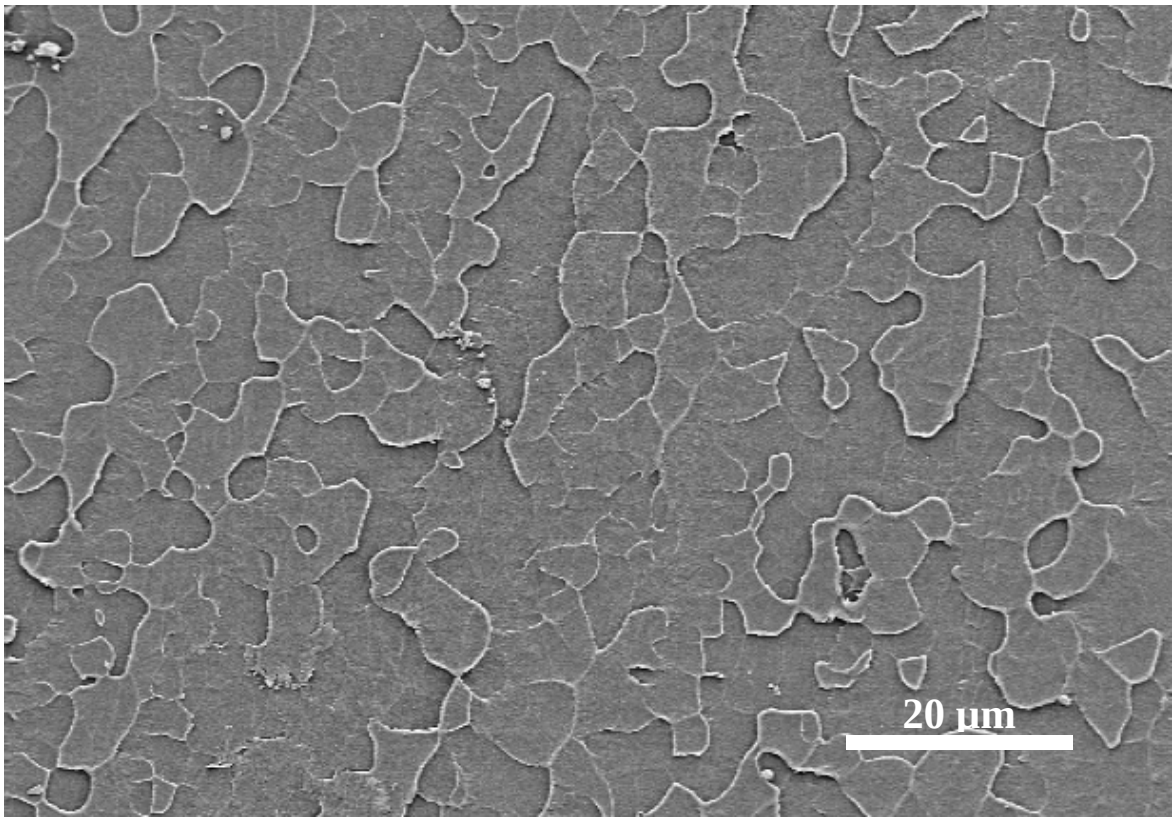

Figure 1a: 25/75 % (v/v) [Purac] PLLA/PMMA composite, sectioned perpendicular to extrusion axis, cryogenic fractured, unetched, gold coated, 4 kV

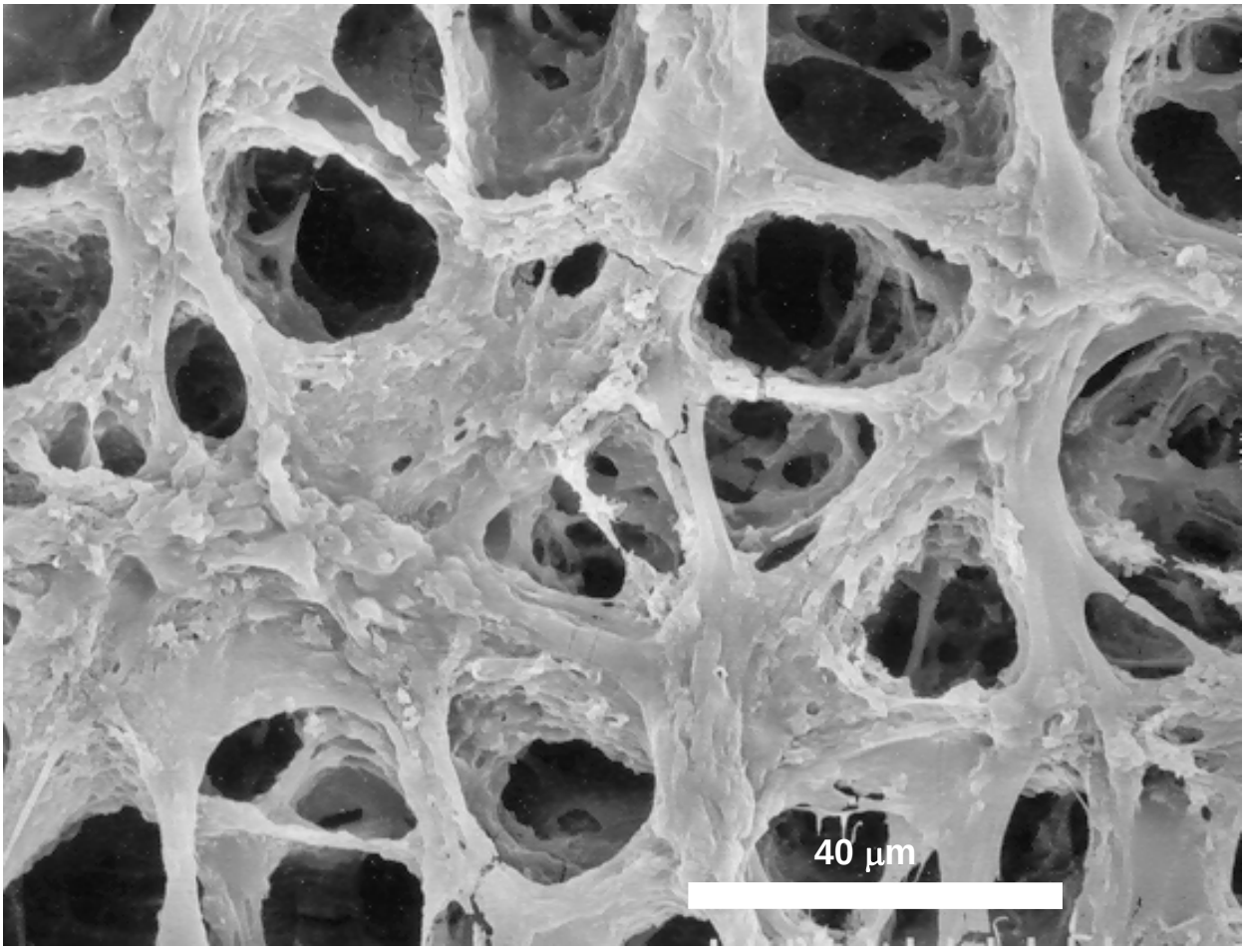

Figure 1b: 28/72 % (v/v) PLLA/PMMA composite; DMF etched, sectioned perpendicular to extrusion axis

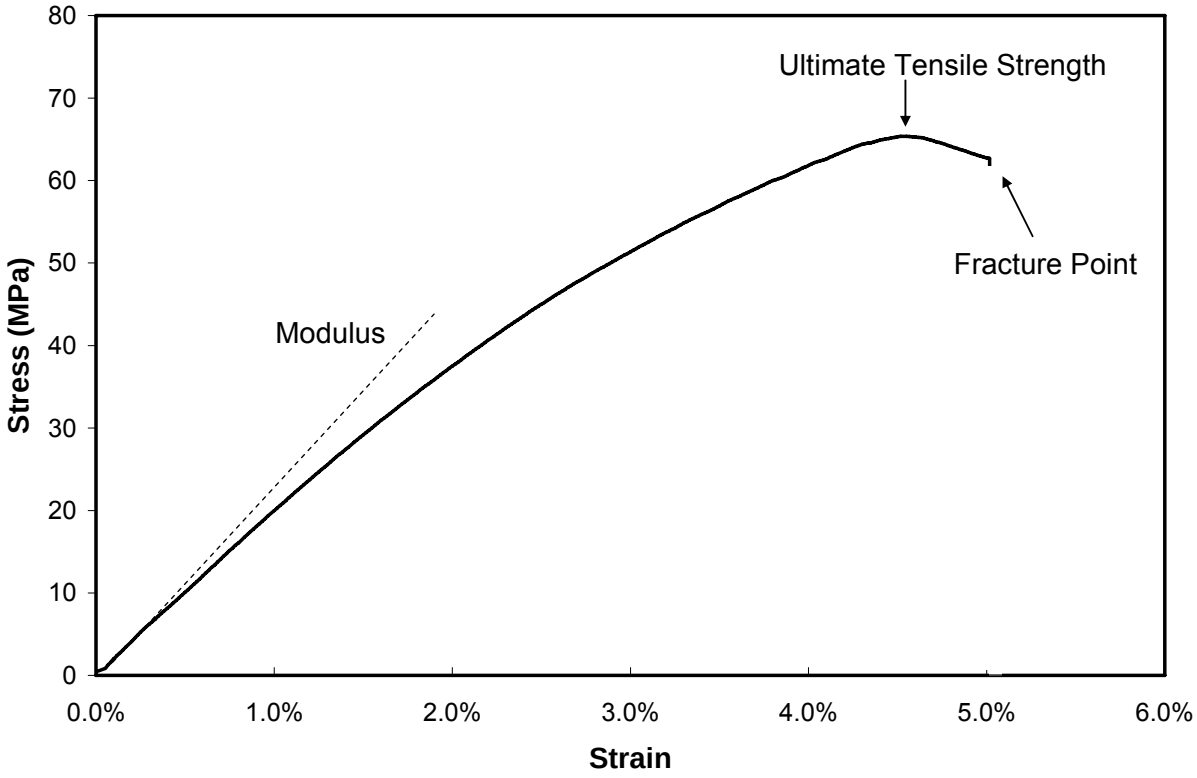

Figure 2a. Representative tensile stress-strain curve for PLLA/PMMA film specimens. This curve is for 60% PLLA by volume.

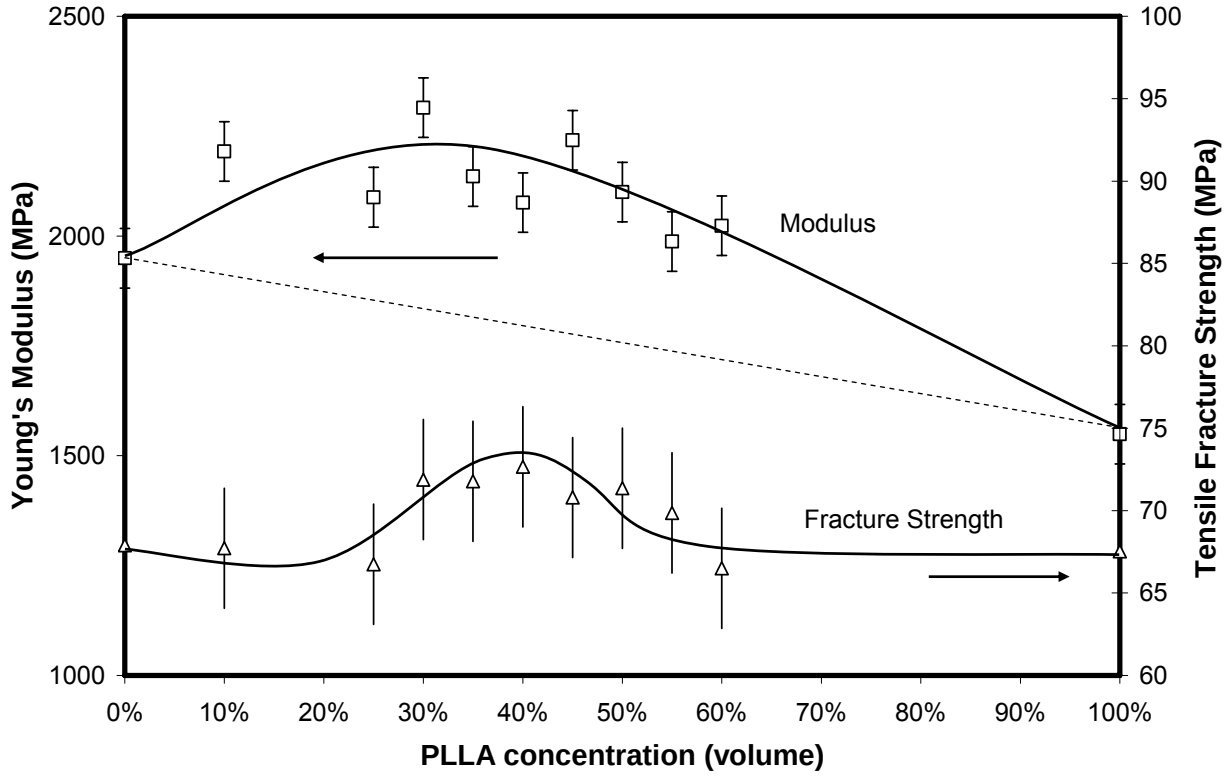

Figure 2b: Tensile modulus and fracture strength of PLLA/PMMA blends. Error bars are Least Significant Difference at 95% confidence interval, degree of freedom *df* = 4.

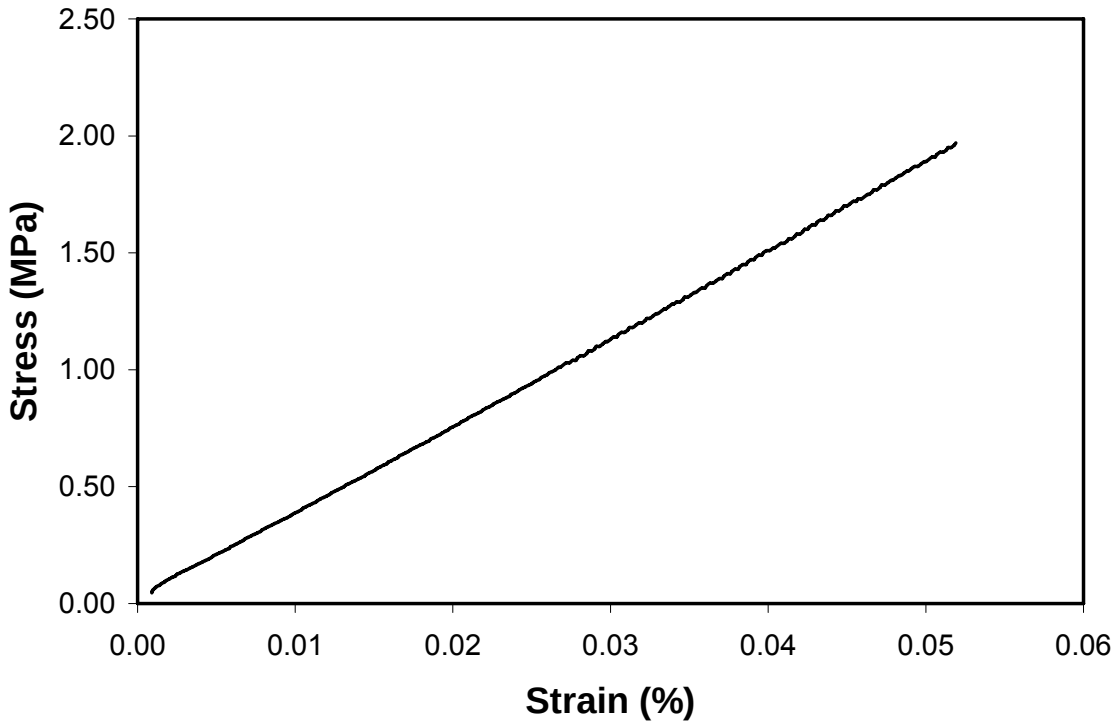

Figure 3a. Representative flexural stress-strain curve for PLLA/PMMA rod specimens. This curve is from 50% blend

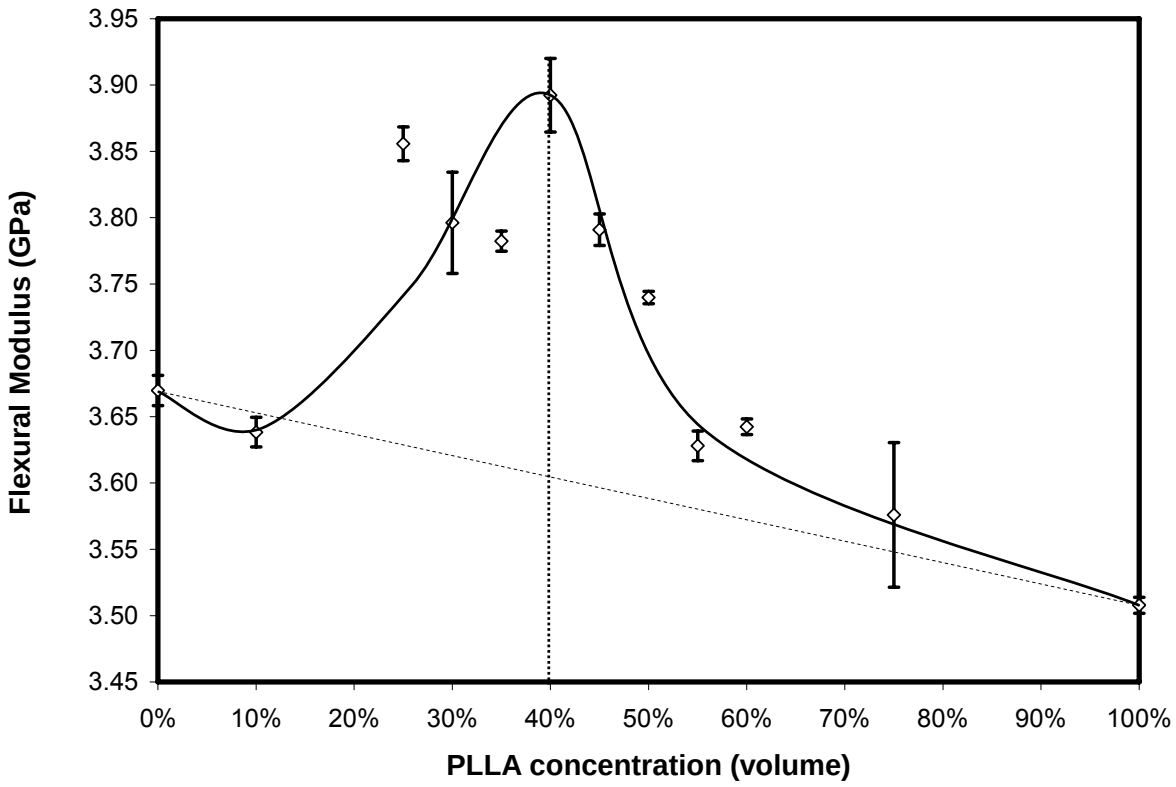

Figure 3b. Flexural modulus of PLLA/PMMA blends from 3-point bending on extruded rods.

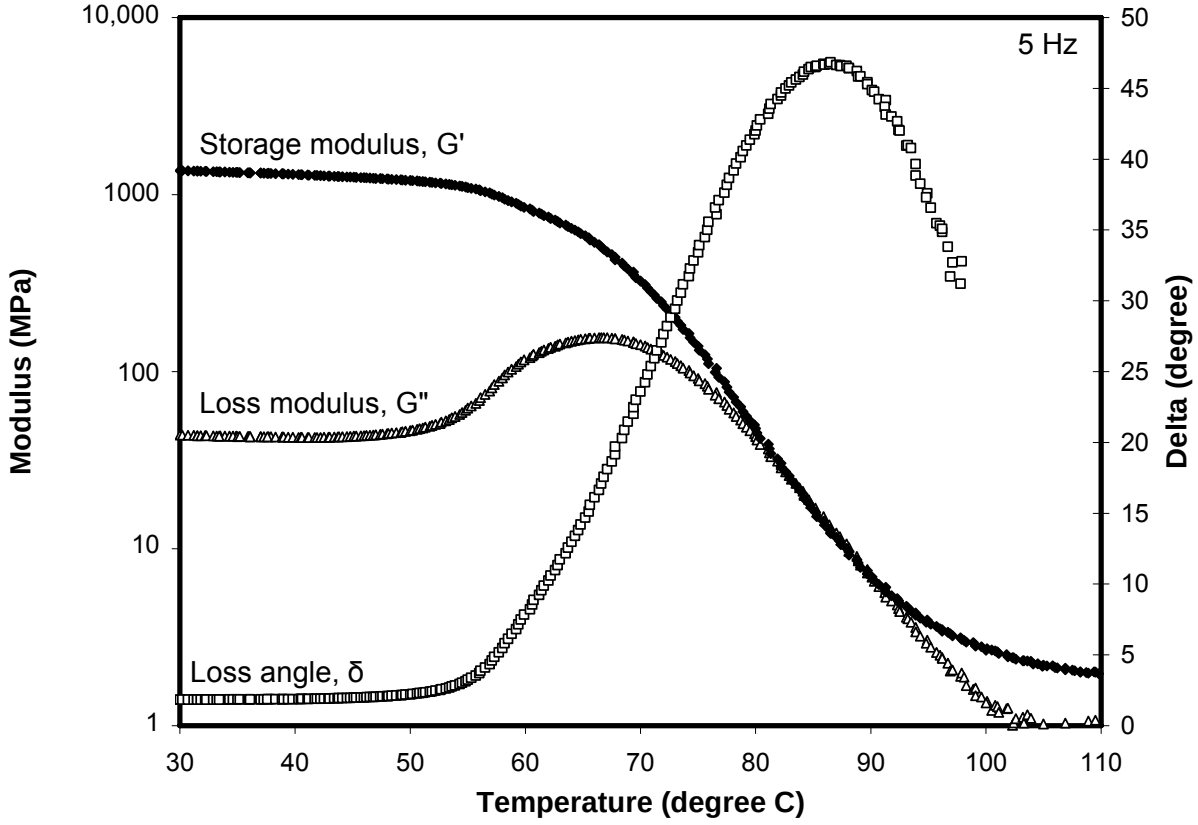

Figure 4a: Modulus and loss angle curves by torsional DMA at 5 Hz for 45/55 PLLA/PMMA blend.

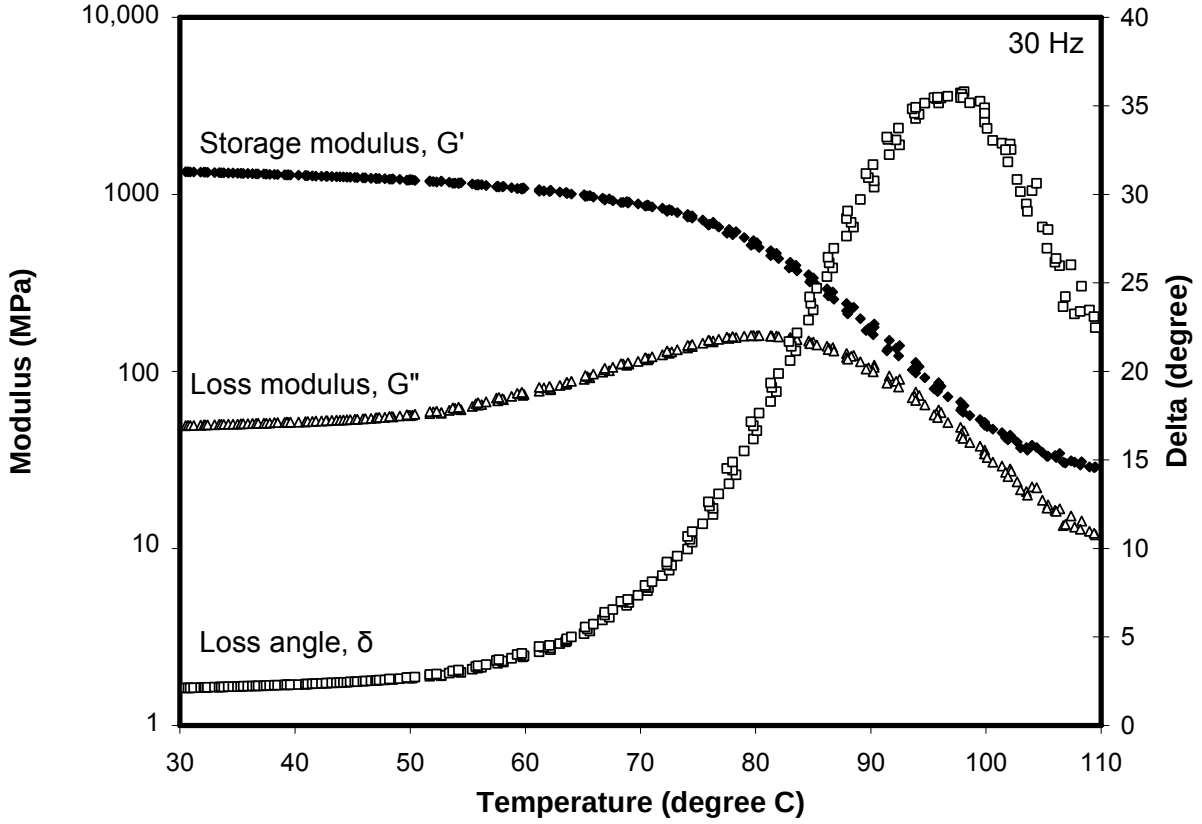

Figure 4b: Modulus and loss angle curves by torsional DMA at 30 Hz for 45/55 PLLA/PMMA blend.

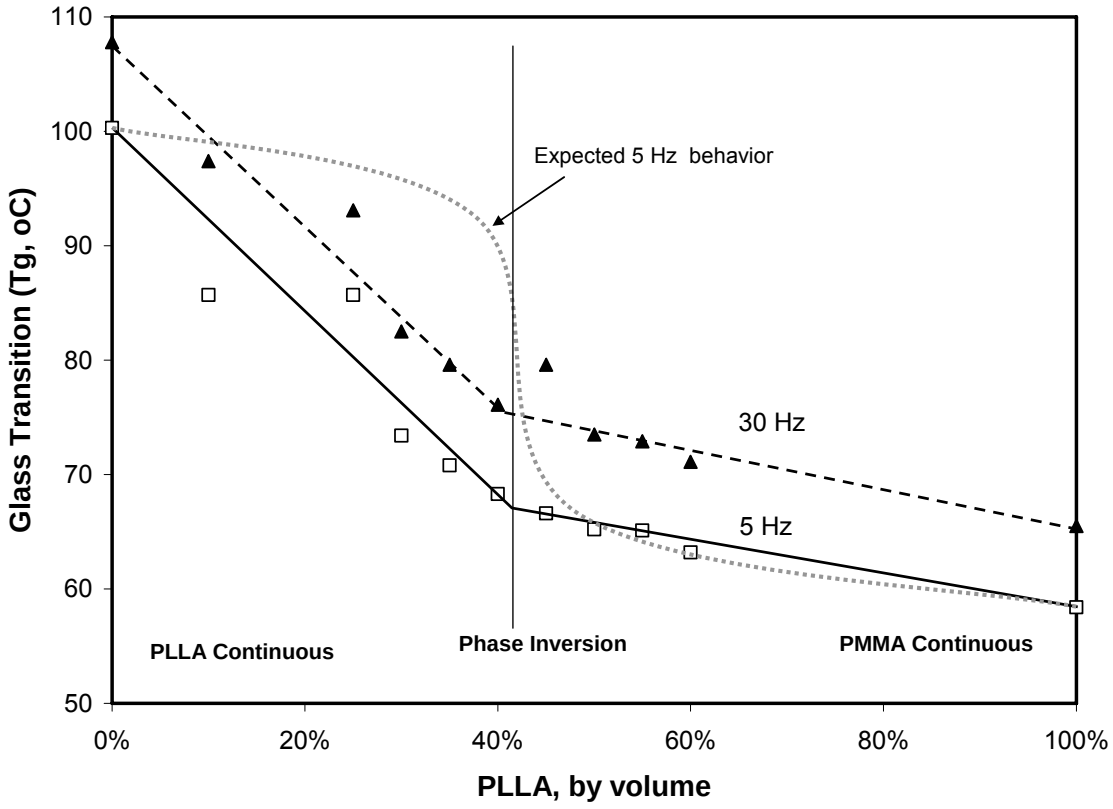

Figure 5: Glass transition of blends as measured by torsional DMA

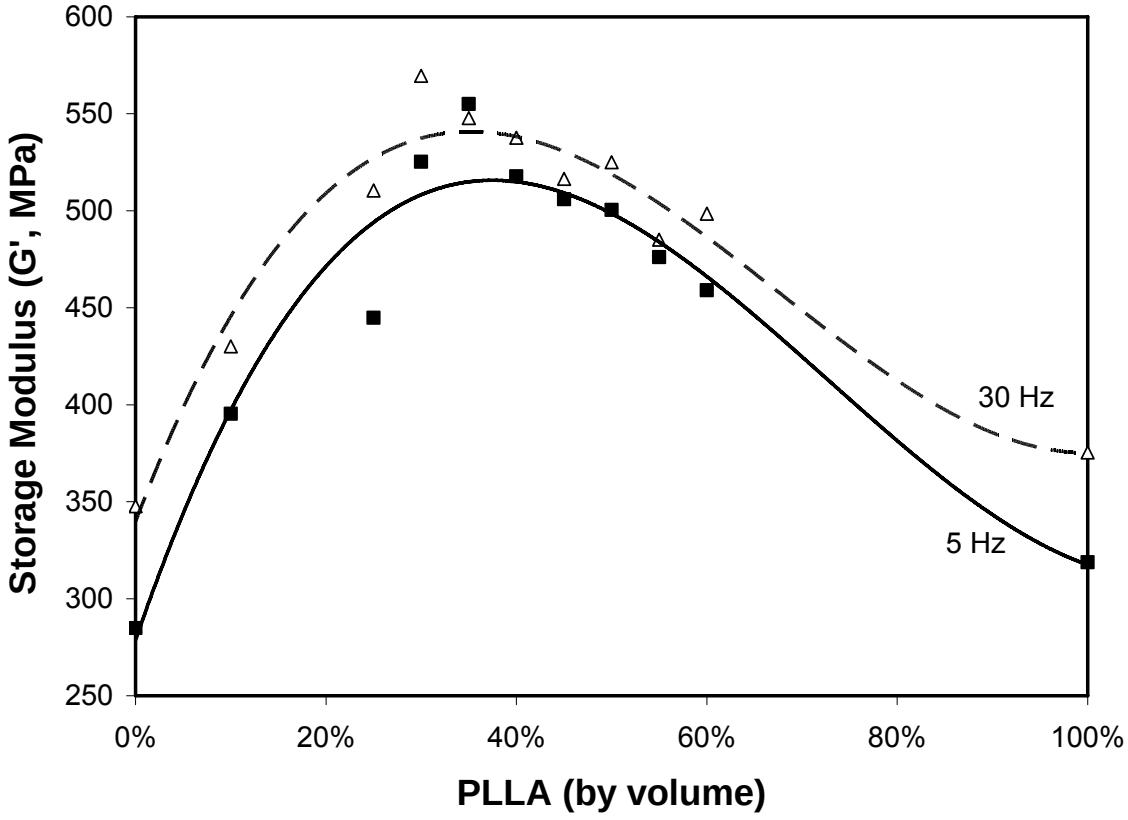

Figure 6a: Storage modulus of PLLA/PMMA blends at the glass transition.

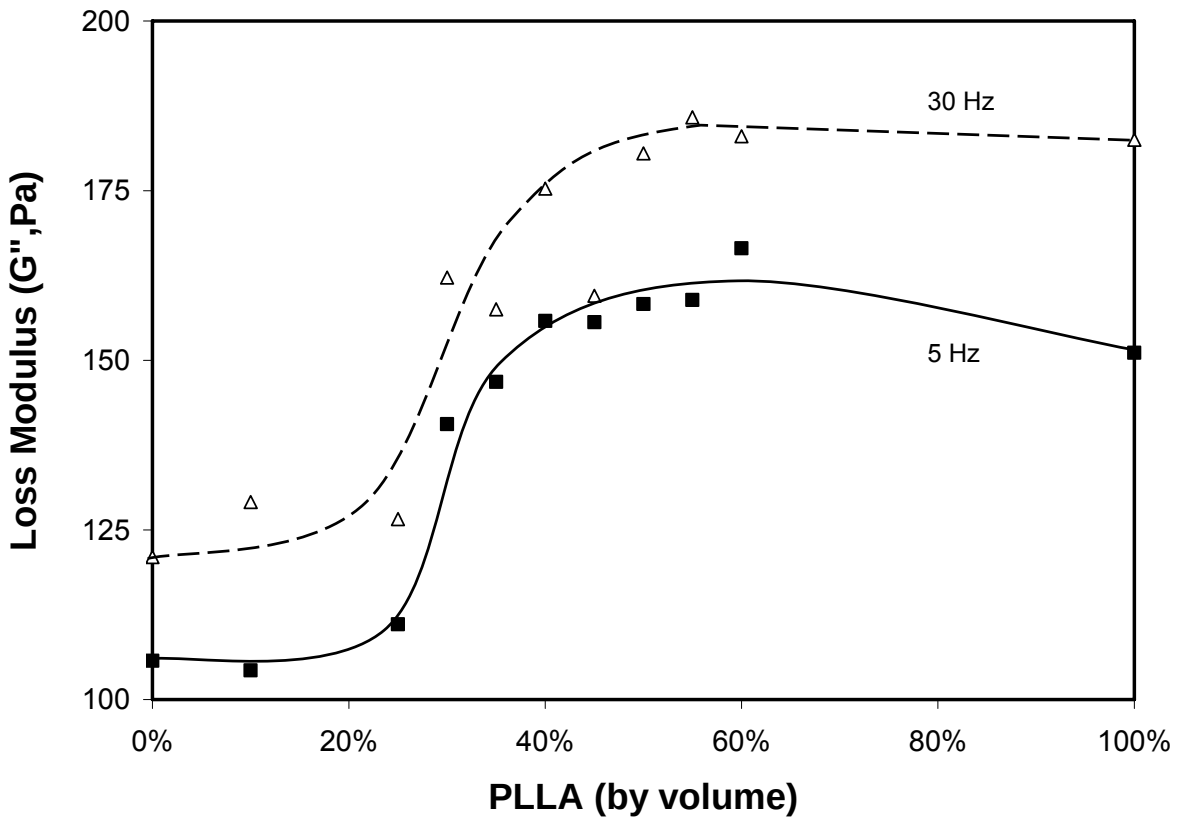

Figure 6b: Loss modulus of PLLA/PMMA blends at the glass transition.

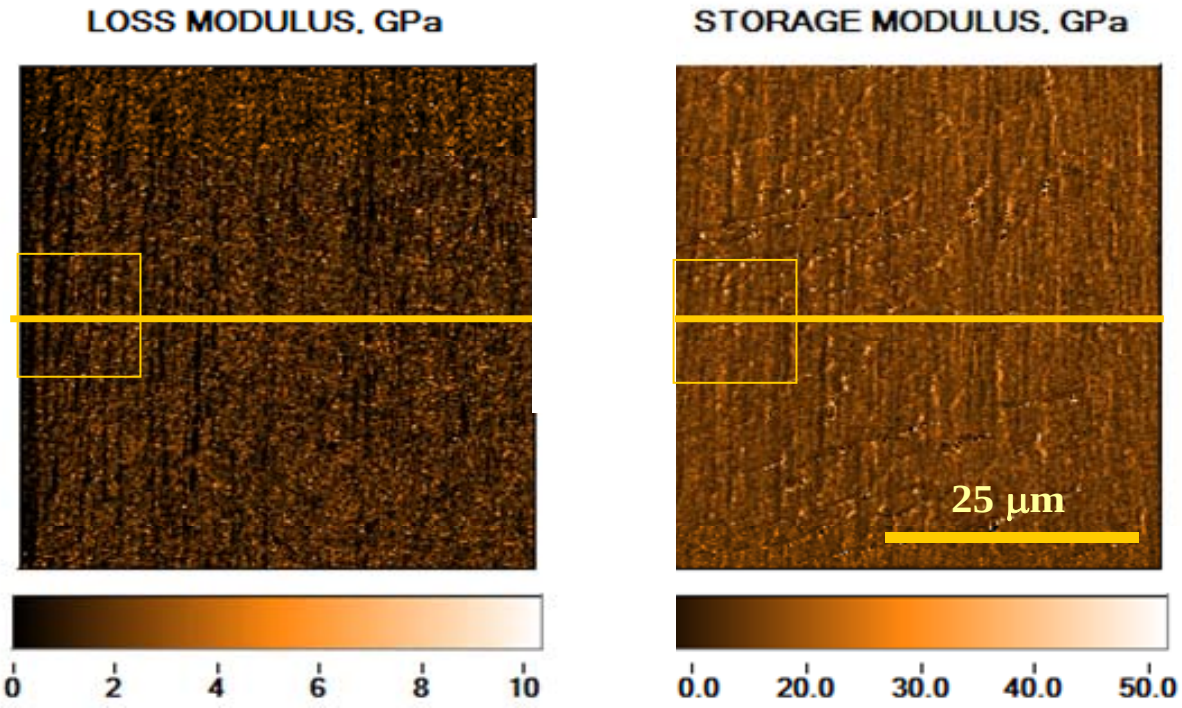

Figure 7a. Loss modulus map by nanoindentation on clean polished cross session of extruded polymer blend rod, 35% PLLA by volume. Dark areas are low modulus, bright areas are high. Line is location of line scan in figure 7b and the 12 μm square is the area of enlargement in 7b.

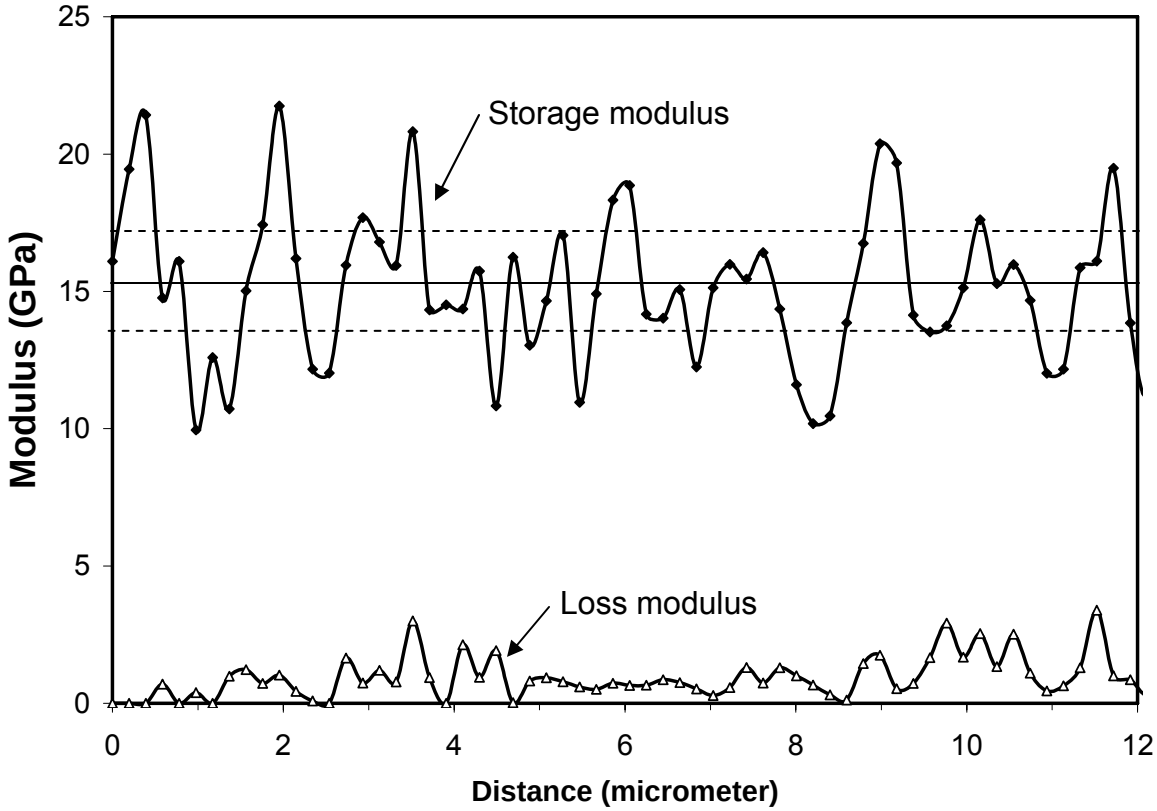

Figure 7b. Modulus line scan from location shown in 7a. Solid horizontal line is mean storage modulus and dotted lines are ±12%

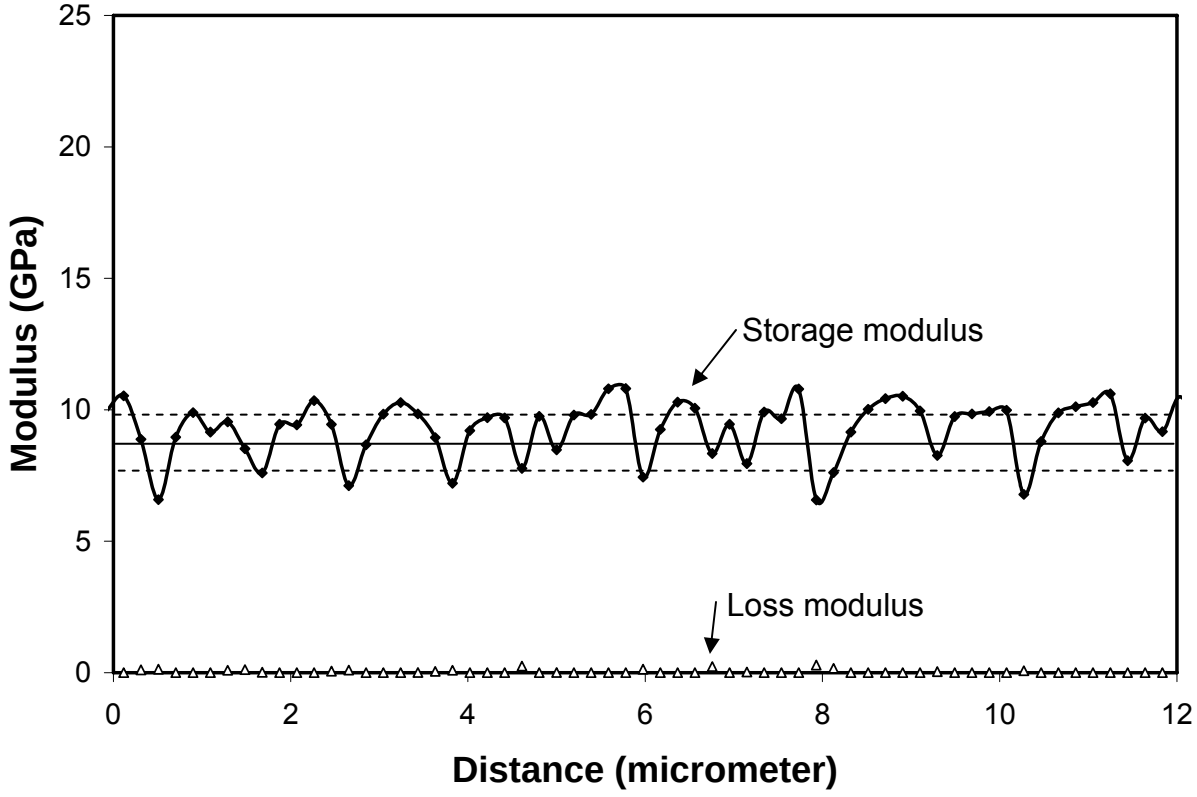

Figure 7c. Modulus line scan for neat PMMA control. Solid horizontal line is mean storage modulus and dotted lines are ±12%.